2018

A conserved circadian function for the Neurofibromatosis 1 gene

Lei Bai
University of Pennsylvania

Yool Lee
University of Pennsylvania

Cynthia T. Hsu
University of Pennsylvania

Julie A. Williams
University of Pennsylvania

Daniel Cavanaugh
University of Pennsylvania

See next page for additional authors

Report

Cell Reports

A Conserved Circadian Function for the *Neurofibromatosis 1* Gene

Graphical Abstract

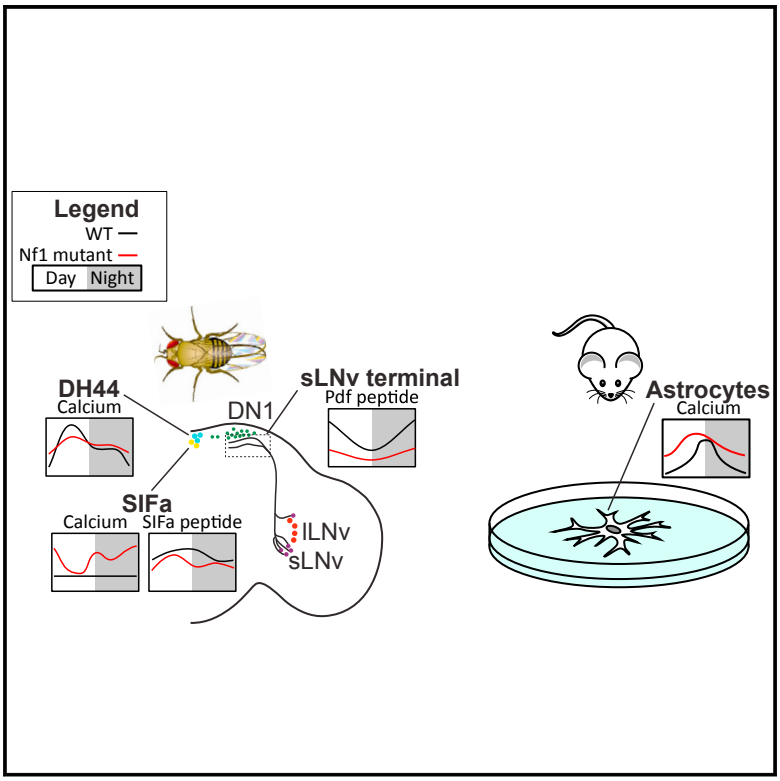

Authors

Lei Bai, Yool Lee, Cynthia T. Hsu, ..., Han Wang, David H. Gutmann, Amita Sehgal

Correspondence

amita@pennmedicine.upenn.edu

In Brief

Bai et al. show that the gene mutated in the disease *Neurofibromatosis 1* is required for maintaining levels or cycling of calcium in circadian neurons in *Drosophila* and in mammalian cells. These effects likely account for effects of *Nf1* on circadian behavior in *Drosophila* and may be relevant in explaining sleep phenotypes in patients.

Highlights

- Loss of *Nf1* affects calcium levels in a circadian circuit in *Drosophila*
- *Nf1* interacts with peptidergic signaling to influence behavior
- Mammalian astrocytes lacking *Nf1* show dampened cycling of calcium

Bai et al., 2018, Cell Reports *22*, 3416–3426
March 27, 2018
https://doi.org/10.1016/j.celrep.2018.03.014

CellPress

OPEN ACCESS
CellPress

Cell Reports
Report

A Conserved Circadian Function for the *Neurofibromatosis 1* Gene

Lei Bai,[1] Yool Lee,[1] Cynthia T. Hsu,[1] Julie A. Williams,[1] Daniel Cavanaugh,[1,2] Xiangzhong Zheng,[1,3] Carly Stein,[1] Paula Haynes,[1] Han Wang,[1,4] David H. Gutmann,[1,5] and Amita Sehgal[1,6,*]

[1]Penn Chronobiology, Howard Hughes Medical Institute, Perelman School of Medicine, University of Pennsylvania, Philadelphia, PA, USA
[2]Department of Biology, Loyola University, Chicago, IL, USA
[3]Bloomington Stock Center, Indiana University, Bloomington, IN, USA
[4]School of Law, University of California, Los Angeles, Los Angeles, CA, USA
[5]Department of Neurology, Washington University, St. Louis, MO, USA
[6]Lead Contact
*Correspondence: amita@pennmedicine.upenn.edu
https://doi.org/10.1016/j.celrep.2018.03.014

SUMMARY

Loss of the *Neurofibromatosis 1* (*Nf1*) protein, neurofibromin, in *Drosophila* disrupts circadian rhythms of locomotor activity without impairing central clock function, suggesting effects downstream of the clock. However, the relevant cellular mechanisms are not known. Leveraging the discovery of output circuits for locomotor rhythms, we dissected cellular actions of neurofibromin in recently identified substrates. Herein, we show that neurofibromin affects the levels and cycling of calcium in multiple circadian peptidergic neurons. A prominent site of action is the pars intercerebralis (PI), the fly equivalent of the hypothalamus, with cell-autonomous effects of *Nf1* in PI cells that secrete DH44. *Nf1* interacts genetically with peptide signaling to affect circadian behavior. We extended these studies to mammals to demonstrate that mouse astrocytes exhibit a 24-hr rhythm of calcium levels, which is also attenuated by lack of neurofibromin. These findings establish a conserved role for neurofibromin in intracellular signaling rhythms within the nervous system.

INTRODUCTION

The *Neurofibromatosis 1* (*Nf1*) gene, which is mutated in the human disease of the same name, is required for rest:activity rhythms in *Drosophila*. Loss of neurofibromin, the protein product of *Nf1*, renders flies largely arrhythmic, indicating that it serves an important function in the circadian system. Subsequent studies also reported sleep abnormalities in humans with *Nf1* (Johnson et al., 2005; Leschziner et al., 2013; Licis et al., 2013; Maraña Pérez et al., 2015), but these have not been traced to the circadian system, nor have circadian phenotypes been reported in *Nf1* mutant mice despite evidence for altered duration of locomotor activity (Weiss et al., 2017). Mouse *Nf1* mutants are only available as heterozygotes, because complete loss of *Nf1* is lethal in mice; thus, behavioral analysis of the genetic null has not been possible.

Despite their abrogated behavioral rhythms, *Drosophila* homozygous *Nf1* mutants show normal cycling of key circadian clock proteins, period (PER) and timeless (TIM), in central clock cells, indicating that output from the clock is affected (Williams et al., 2001). Consistent with the known function of mammalian neurofibromin as a Ras-GTPase-activating protein (Ras-GAP), effects of *Drosophila Nf1* on rest:activity rhythms are mediated by increased Ras/mitogen-activated protein kinase (MAPK) pathway signaling (Williams et al., 2001). However, we still have no understanding of the mechanisms by which *Nf1* affects transmission of time-of-day signals from the clock.

Identification of a circadian output circuit provides a unique opportunity to assess the effects of *Nf1* on cellular function within cells downstream of the clock. In this circuit, the central clock cells, small ventral lateral neurons (sLNvs), signal via a neuropeptide, pigment-dispersing factor (PDF), to a dorsally located clock neuron cluster, DN1, which in turn connects to non-clock cells in the pars intercerebralis (PI) (Cavanaugh et al., 2014). The PI is the fly equivalent of the hypothalamus and consists of multiple groups of peptidergic neurons, some of which modulate rest:activity rhythms while others regulate metabolic rhythms (Barber et al., 2016; Cavanaugh et al., 2014). The clusters that express the diuretic hormone 44 (DH44) and *Drosophila* neuropeptide AYRKPPFNGSIFamide (SIFamide) peptides, respectively, are important for rest:activity rhythms (Cavanaugh et al., 2014).

Here, we report that *Nf1* is required broadly within the *Drosophila* circadian circuit for rest:activity rhythms and, consistent with that requirement, affects cellular function in multiple neuronal populations. Specifically, loss of *Nf1* impairs rhythms of intracellular calcium, a correlate of neural activity, as well as peptide expression in subsets of circadian neurons. Reduction of *Nf1* partially rescues rhythms in a PDF receptor mutant, indicating that interactions between neurofibromin and peptide signaling are relevant for behavioral rhythms. As noted earlier, the lethality associated with loss of *Nf1* in mice has thus far impeded assessment of its contribution to circadian regulation. The identification of a cellular endpoint of *Nf1* disruption in flies also allowed us to assay the effect of *Nf1* loss in mammalian cells, specifically mouse astrocytes that are known to be a site of neurofibromin action (Smithson and Gutmann, 2016). We find that calcium levels are rhythmic over a 24-hr day in wild-type astrocytes, but the cycling is dampened in *Nf1*-deficient

astrocytes, which exhibit a general elevation in calcium. Altogether, these findings establish a conserved role for neurofibromin in the regulation of daily rhythms.

RESULTS

Neurofibromin Is Required Broadly in the *Drosophila* Brain for Rest:Activity Rhythms

We first sought to identify the anatomical location that mediates effects of *Nf1* on circadian rhythms. Earlier work, using the upstream activating sequence (UAS)-GAL4 system to target *Nf1* expression, indicated that neurofibromin expression in clock neurons was not sufficient for rest:activity rhythms (Williams et al., 2001). Other sites, or perhaps even multiple locations, of action were indicated, which is supported by the finding that *Nf1* is expressed broadly across the adult fly brain (Buchanan and Davis, 2010). Thus, we went beyond the clock cell drivers used in the previous study and assayed for rescue of the mutant phenotype following *Nf1* expression in different neuronal populations of *Nf1* homozygous mutant flies. We found that behavioral rhythms were restored when *Nf1* expression was driven by GAL4 drivers expressed broadly, such as the pan-neuronal synaptobrevin-GAL4 driver or the Cha-GAL4 driver expressed in all cholinergic cells (Table 1). Because most adult fly brain neurons are cholinergic (Gorczyca and Hall, 1987), rescue with the Cha driver does not implicate any specific brain region. In addition, the c309-GAL4 and 53b-GAL4 drivers that are expressed in multiple brain regions yielded partial rescue (Table 1).

Consistent with previous findings (Williams et al., 2001), neither the *Pdf*-GAL4 driver, expressed specifically in ventral lateral neurons (LNvs), nor the *Clk*4.1-GAL4 driver, which targets DN1s (Guo et al., 2016), rescued the *Nf1* mutant phenotype. Rescue was also not seen with expression targeted to monoaminergic cells using the *ddc*-GAL4 and *Tdc2*-GAL4 drivers. Even the c929-GAL4 driver, which is expressed in most peptidergic cells, including those of the PI (Hewes et al., 2000), did not rescue the *Nf1* mutant phenotype. These results suggest that neurofibromin is required in more than one location for rest:activity rhythms. However, we acknowledge that negative results with some drivers may be due to the reduced strength of these drivers.

Because the rescuing drivers (e.g., synaptobrevin and Cha-GAL4) are expressed at developmental stages, in addition to the adult stage, we asked whether *Nf1* is required in adults for normal rest:activity rhythms. We drove expression of *Nf1* RNAi with a pan-neuronally expressed and RU-486 inducible driver, synaptobrevin GeneSwitch (nsyb-GS), and knocked down expression specifically in adults by feeding flies RU-486. Knockdown in adults also reduced rhythm strength, although not to the extent seen in *Nf1* mutants (Figure S1). The weaker phenotype could reflect incomplete knockdown by RNAi or an additional role in development. Nevertheless, these data indicate that *Nf1* functions in adults to maintain circadian behavior.

Neurofibromin Function in Circadian Clock Neurons

Given the rather broad requirement for neurofibromin in the generation of circadian behavioral rhythms, we sought to address its impact in different cells of the circadian circuit important for rest:activity rhythms. We started with the LNvs, which express the PDF neuropeptide. Circadian clock proteins were shown to cycle in LNvs of *Nf1* mutant flies (Williams et al., 2001), so we examined effects of neurofibromin loss on rhythmic outputs of these neurons. PDF is the major output of these neurons, and its expression is rhythmic at the terminus of the dorsal projection from the sLNvs (Park et al., 2000). To determine whether this rhythm in PDF expression is intact in *Nf1* mutants, we examined expression at times of low and high expression, circadian time (CT) 1 and 13, respectively, in flies maintained in constant darkness (DD) following entrainment to light:dark cycles. Whereas wild-type flies showed a cyclic pattern (Park et al., 2000), PDF expression did not change between time points at the dorsal terminus in *Nf1* mutants and was constantly low (Figure 1).

Because reduced accumulation of PDF at the axon terminal is thought to indicate increased peptide release (Park et al., 2000), PDF signaling might be increased in *Nf1* mutants. We hypothesized that if *Nf1* mutants have increased PDF release, then this could be counteracted by reducing expression of the PDF receptor (PDFR). To test this idea, we generated double mutants of *Nf1* loss coupled with each of two mutant alleles of the PDF receptor, *pdfr*. Like *Nf1* mutants, mutants of PDF or of its receptor are largely arrhythmic, although the limited rhythmic flies show a short period (Hyun et al., 2005; Lear et al., 2005; Mertens et al., 2005).

We were unable to rescue rest:activity rhythms of *Nf1* homozygous mutants with hypomorphic alleles of *pdfr*, tested as heterozygotes or homozygotes. This is perhaps not surprising, given that *pdfr* action in circadian behavior maps to specific neurons, largely the clock network (Im and Taghert, 2010), while neurofibromin, as demonstrated earlier, is required broadly. *Nf1* not only is required broadly but also affects multiple circadian cells (described later). However, loss of one copy of *Nf1* rescued the short period of both *pdfr* mutants and partially rescued rhythmicity in one of the two mutant lines (Table 2). Thus, neurofibromin and PDF interact genetically in the generation of behavioral rhythms.

Small LNvs project to DN1 clock cells, which are part of the circuit required for rest:activity rhythms. To determine whether neurofibromin affects the clock or clock output in DN1s, we first examined the expression of the PER clock protein at different times of day in constant darkness. In *Nf1* mutants, as in wild-type flies, PER expression was cyclic, peaking at CT1 and nadiring at CT13 (Figure S2). In the absence of an established molecular assay for rhythmic output in these cells, we measured calcium using a CaLexA reporter (Masuyama et al., 2012). Calcium levels were rhythmic in a subset of DN1s, even in constant darkness following entrainment to light:dark cycles, and the rhythm was evident in both wild-type flies and *Nf1* mutants (Figure S2). In addition, we did not detect changes in overall calcium levels in *Nf1* mutants relative to wild-type controls. We conclude that neurofibromin has limited, if any, effects on DN1s.

Neurofibromin Affects Neural Activity in PI Cells that Secrete DH44

Although cells in the PI do not contain clocks, they receive input from upstream DN1s and are required for different circadian outputs (Barber et al., 2016; Cavanaugh et al., 2014). DH44-positive

Table 1. Rescue of Rhythms in *Nf1* Mutants by Restoring NF1 in Subsets of Neurons

Genotype	R (%) (n)	Period ± SEM (hr)	FFT ± SEM
n-syb-Gal4/+;*UAS-Nf1*,$Nf1^{P1}$/$Nf1^{P2}$	100 (18/18)	23.78 ± 0.16	0.050 ± 0.006
n-syb-Gal4/+;$Nf1^{P1/P2}$	0 (0/22)		
Cha-Gal4/+;*UAS-Nf1*,$Nf1^{P1}$/$Nf1^{P2}$	100 (20/20)	23.77 ± 0.10	0.067 ± 0.008
Cha-Gal4/+;$Nf1^{P1/P2}$	4.3 (1/23)	23.75	0.03
Ddc-Gal4/+;*UAS-Nf1*,$Nf1^{P1}$/$Nf1^{P2}$	7.7 (1/13)	23	0.02
Ddc-Gal4/+;$Nf1^{P1/P2}$	0 (0/13)		
Tdc-Gal4/+;*UAS-Nf1*,$Nf1^{P1}$/$Nf1^{P2}$	2.8 (3/36)	23.67 ± 0.21	0.023 ± 0.003
Tdc-Gal4/+;$Nf1^{P1/p2}$	0 (0/10)		
C453/+;*UAS-Nf1*,$Nf1^{P1}$/$Nf1^{P2}$	19.0 (4/21)	24.12 ± 0.27	0.025 ± 0.006
C453/+;$Nf1^{P1/P2}$	0 (0/13)		
1471/+;*UAS-Nf1*,$Nf1^{P1}$/$Nf1^{P2}$	11.1 (2/18)	24.58 ± 2.08	0.03 ± 0.01
1471/+;$Nf1^{P1/P2}$	0 (0/13)		
201y/+;*UAS-Nf1*,$Nf1^{P1}$/$Nf1^{P2}$	0 (0/32)		
201y/+;$Nf1^{P1/P2}$	0 (0/7)		
C309/+;*UAS-Nf1*,$Nf1^{P1}$/$Nf1^{P2}$	50 (13/26)	24.10 ± 0.43	0.055 ± 0.006
C309/+;$Nf1^{P1/P2}$	0 (0/10)		
112749/+;*UAS-Nf1*,$Nf1^{P1}$/$Nf1^{P2}$	15.6 (5/32)	24.10 ± 0.36	0.014 ± 0.002
112749/+;$Nf1^{P1/P2}$	0 (0/16)		
53b/+;*UAS-Nf1*,$Nf1^{P1}$/$Nf1^{P2}$	57.1 (16/28)	24.06 ± 0.21	0.024 ± 0.005
53b/+;$Nf1^{P1/P2}$	0 (0/13)		
C739/+;*UAS-Nf1*,$Nf1^{P1}$/$Nf1^{P2}$	0 (0/16)		
C739/+;$Nf1^{P1/P2}$	0 (0/3)		
C929/+;*UAS-Nf1*,$Nf1^{P1}$/$Nf1^{P2}$	0 (0/17)		
C929/+;$Nf1^{P1/P2}$	0 (0/11)		
MJ63/+;*UAS-Nf1*,$Nf1^{P1}$/$Nf1^{P2}$	23.1 (3/13)	23.83 ± 0.25	0.017 ± 0.007
MJ63/+;$Nf1^{P1/P2}$	0 (0/14)		
Kurs58/+;*UAS-Nf1*,$Nf1^{P1}$/$Nf1^{P2}$	25.0 (4/16)	22.96 ± 0.10	0.015 ± 0.04
Kurs58/+;$Nf1^{P1/P2}$	8.7 (2/23)	23.74 ± 0.23	0.030 ± 0.07
*Clk*4.1 m/+;*UAS-Nf1*,$Nf1^{P1}$/$Nf1^{P2}$	8.0 (2/25)	23.57 ± 0.20	0.032 ± 0.004
*Clk*4.1 m/+;$Nf1^{P1/P2}$	4.5 (1/22)	23.92	0.029
InSITE911/+;*UAS-Nf1*,$Nf1^{P1}$/$Nf1^{P2}$	0 (0/6)		
InSITE911/+;$Nf1^{P1/P2}$	0 (0/11)		
121y/+;*UAS-Nf1*,$Nf1^{P1}$/$Nf1^{P2}$	8.3 (1/12)	23.83	0.036
121y/+;$Nf1^{P1/P2}$	0 (0/4)		
Pdf-G4/+;*UAS-Nf1*,$Nf1^{P1}$/$Nf1^{P2}$	7.6 (1/13)	23.33	0.011
Pdf-G4/+;$Nf1^{P1/P2}$	0 (0/13)		
UAS-Nf1,$Nf1^{P1}$/$Nf1^{P2}$	8.9 (2/23)	23.46 ± 0.13	0.002 ± 0.000

See Figure S1 for adult-specific effects of *Nf1* knockdown. Flies showing a fast Fourier transform (FFT) value >0.01 are counted as rhythmic (R). The average periods and FFTs shown represent the means ± SEM for all rhythmic flies. FFT values were calculated for the first 7 days in constant darkness.

neurons in the PI are particularly important for the regulation of rest:activity rhythms (Cavanaugh et al., 2014). To assess a possible role for neurofibromin in these cells, we initially assayed DH44 expression in *Nf1* mutants. Because DH44 expression does not cycle, we examined a single time point in the presence of light:dark cycles (zeitgeber time 13 [ZT13]) and in constant darkness (CT13) and found that overall expression of DH44 was not different between wild-type flies and *Nf1* mutants (Figure 2A) (data not shown). However, this did not preclude an effect of neurofibromin on rhythmic output in these cells, which we then assayed by measuring calcium as a proxy for neural activity. As previously reported with a different calcium sensor (Cavey et al., 2016), the CaLexA reporter revealed a rhythm of calcium in these cells, showing significantly higher levels at ZT13 than at ZT1 (Figure 2B). No such rhythm was seen for calcium in *Nf1* mutants, suggesting that neurofibromin is required for rhythmic output from DH44 cells.

Because cellular rhythms were normal in DN1 neurons, which are upstream of DH44 cells in the circadian circuit, we surmised that neurofibromin had independent effects in DH44 cells. To

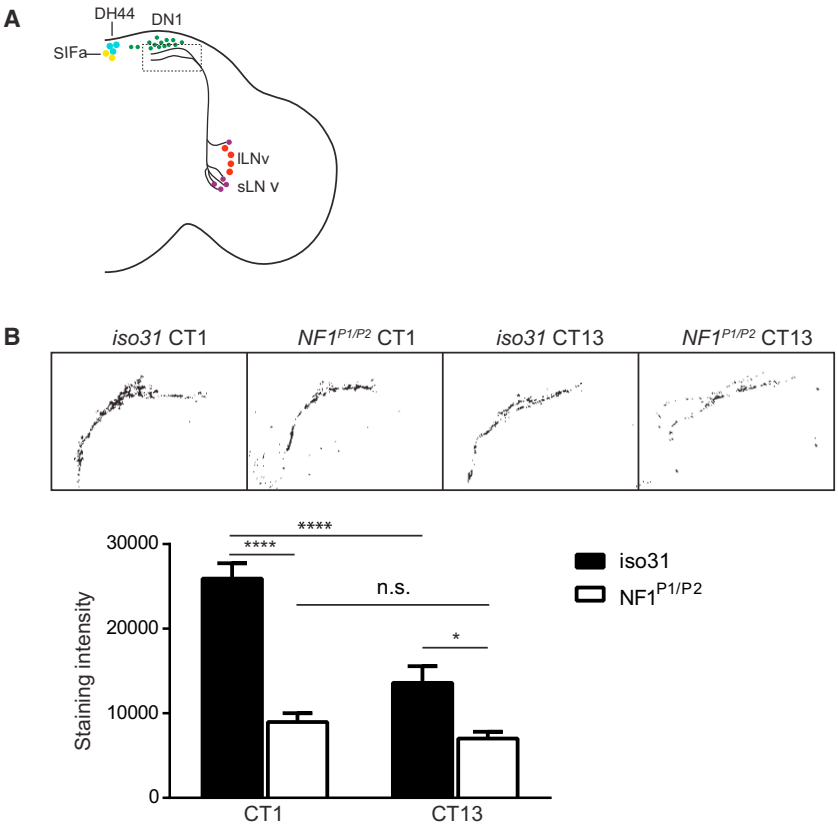

Figure 1. PDF Accumulation Is Reduced in the Dorsal Brain in *Nf1* Mutants

(A) Schematic drawing of the fly brain showing the circadian circuit for locomotor rhythms, which includes the master pacemaker s-LNvs (magenta), DN1 clock cells (green), and DH44+ (cyan) and SIFa+ (yellow) cells in the PI. The dashed box shows the region of the dorsal brain imaged in (B).

(B) PDF staining in the dorsal termini of s-LNvs at CT1 and CT13 in *iso31* and $Nf1^{P1/P2}$ mutant flies. CT, circadian time. Representative images are shown in the top panel. Quantification of average staining intensity (mean ± SEM) is shown in the bottom panel. ****$p < 0.0001$, *$p < 0.05$ (one-way ANOVA and Tukey's multiple comparison test). n = 14 brains for *iso31* CT1, *iso31* CT13, and *Nf1* CT1, and n = 11 brains for *Nf1* CT13. See Figure S2 for analysis of DN1 neurons.

determine whether the effect was cell autonomous, we attempted to rescue the phenotype in DH44 cells by expressing *Nf1* specifically in these cells in a mutant background. Calcium cycling was restored in flies expressing *Nf1* in DH44 cells, while controls that contained the *Nf1* mutation, but only with the Gal4 transgene and not UAS-*Nf1*, remained arrhythmic. These data indicate that neurofibromin acts in DH44 cells to affect rhythms of calcium.

Neurofibromin Affects Neural Activity in PI Cells that Secrete SIFamide

SIFamide (SIFa) is expressed in four PI cells, which are also required for rest:activity rhythms (Cavanaugh et al., 2014). We found that *Nf1* loss dramatically increased *SIFa* mRNA levels (Figure 3A), albeit with a small decrease in the corresponding protein levels as detected in projections throughout the brain (Figures 3B and 3C). Neither RNA nor protein expression was found to cycle, and we did not detect a rhythm in neural activity via calcium imaging. However, *Nf1* mutants showed robust increases in calcium levels in SIFa-producing cells, which is likely indicative of increased release and may account for reduced accumulation of protein (Figures 3D and 3E) (Kwon et al., 2015; Park et al., 2000). The strongest influence of neurofibromin loss was observed in SIFa-producing cells. As in the case of DH44 cells, the effects of *Nf1* in SIFa cells are likely cell autonomous and independent of those in other circadian cells.

Given the dramatic effects of the *Nf1* mutation on *SIFa* gene expression and SIFa cell activity, we sought to determine whether SIFa contributes to neurofibromin regulation of behavioral rhythms. Although SIFa cells are implicated in circadian rhythms (Cavanaugh et al., 2014), a role for the peptide has not been tested. To examine this potential role, we generated a *SIFa* mutant by CRISPR/Cas9 genome editing and tested it for circadian rest:activity rhythms. Three independent mutant lines were obtained, and although we observed a small reduction in rhythm strength, this was not consistent across lines and in mutant-deficiency combinations. These results indicate that SIFa is not a major contributor to rest:activity rhythms (Table 3), even though the cells that produce it are important.

SIFa is also implicated in the regulation of sleep (Park et al., 2014), as is *Nf1* (Bai and Sehgal, 2015). It is unclear whether effects of *Nf1* on sleep are related to its effects on circadian rhythms, but overlapping mechanisms are a distinct possibility given that several circadian neurons have roles in sleep (Artiushin and Sehgal, 2017). We found, as predicted from RNAi analysis (Park et al., 2014), that *SIFa* mutants have reduced sleep (Figure S3), so we asked whether the *Nf1* mutant sleep phenotype is mediated through effects on SIFa expression. We generated double mutants lacking both SIFa and neurofibromin and tested them in sleep assays. Double mutants showed sleep reduction equivalent to that in *Nf1* single mutants (Figure S3B), indicating that these two genes act in the same pathway to regulate sleep (Figure S3).

Neurofibromin Is Required for Calcium Cycling in Mouse Astrocytes

Neurofibromin has not yet been implicated in circadian rhythms in mammals, although it is associated with sleep phenotypes in humans (Johnson et al., 2005; Leschziner et al., 2013; Licis et al., 2013; Maraña Pérez et al., 2015) and with locomotor activity levels in mice (Weiss et al., 2017). Detection of rhythm phenotypes in knockout mice is complicated by the complete *Nf1* loss being embryonic lethal (these mice also frequently show exencephaly) (Lakkis et al., 1999), and effects of the mutation may be

Table 2. *Nf1*^{P1} Rescues the Short Period Phenotype of the *pdfr* Mutant

Genotype	N	SR (%)	MR (%)	WR (%)	AR (%)	FFT ± SEM	Period ± SEM (hr)
iso31	64	87.5	9.4	1.6	1.6	0.089 ± 0.004	23.79 ± 0.10
Nf1^{P1}/+	62	48.4	33.9	9.7	8.1	0.065 ± 0.004*	23.72 ± 0.08
pdfr^{33068}/Y	32	3.1	9.4	43.8	43.8	0.026 ± 0.012****	22.63 ± 0.15****
pdfr^{33069}/Y	31	3.2	9.7	32.3	54.8	0.025 ± 0.013****	22.83 ± 0.22****
pdfr^{33068}/Y;*Nf1*^{P1}/+	32	0.0	15.6	43.8	40.6	0.022 ± 0.010****	23.57 ± 0.06 NS
pdfr^{33069}/Y;*Nf1*^{P1}/+	30	16.7	16.7	46.7	20.0	0.047 ± 0.009****	23.58 ± 0.06 NS

SR, strongly rhythmic; MR, moderately rhythmic; WR, weakly arrhythmic; AR, arrhythmic. ****p < 0.0001, *p < 0.05; NS, not significant, compared with *iso31*. In addition to period, loss of one copy of *Nf1* partially rescues overall rhythmicity and rhythm strength of the *Pdfr*^{33069} allele.

recessive at the cellular level. Based on the preceding studies that indicated a cellular phenotype in *Nf1* mutant flies, we sought to determine whether a similar abnormal phenotype was manifest in mammalian cells lacking neurofibromin expression. Because we were interested in adult cells and wanted to avoid the lethality associated with neuronal loss, we used mouse brainstem astrocytes in which neurofibromin expression was acutely deleted by Cre-mediated excision (Smithson and Gutmann, 2016). Astrocytes were shown to have an important role in circadian timekeeping in the mammalian central clock, the suprachiasmatic nucleus (SCN), so they are a relevant cell type for this purpose (Barca-Mayo et al., 2017; Brancaccio et al., 2017; Tso et al., 2017).

Circadian rhythms can be studied in cultured cells by synchronizing clocks across cells with a stimulus like dexamethasone, which is a synthetic glucocorticoid (Balsalobre et al., 2000); dexamethasone was even used to assay circadian cycling in astrocytes (Barca-Mayo et al., 2017). Typically,

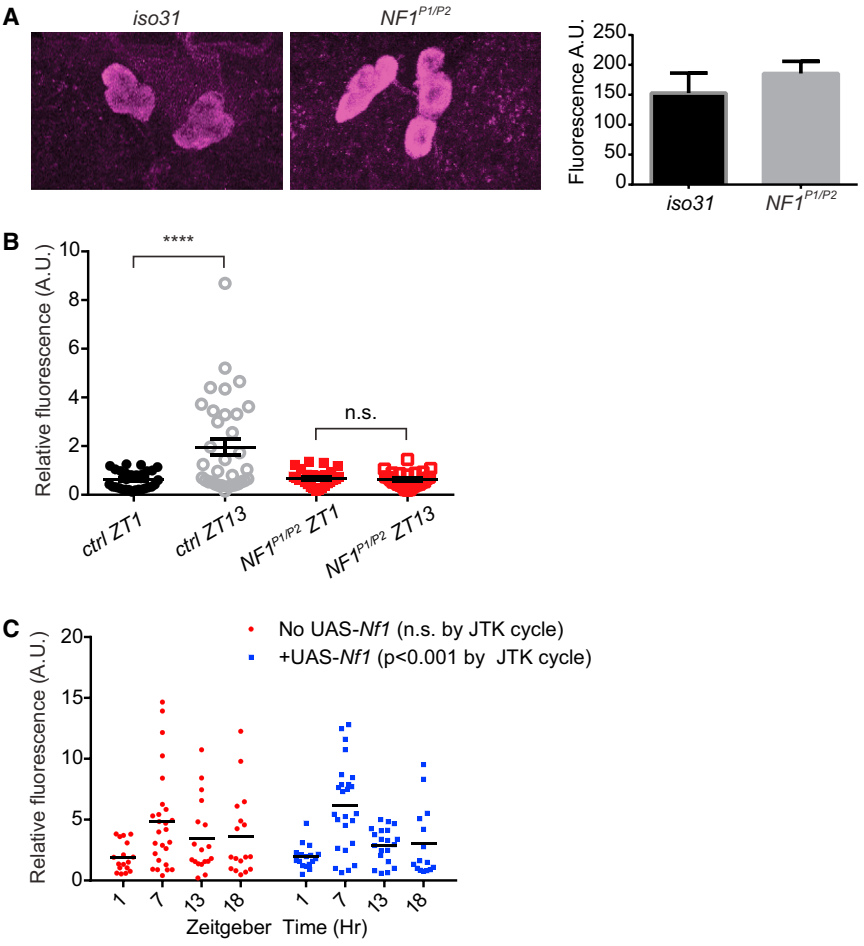

Figure 2. Neurofibromin Has Cell-Autonomous Effects on Rhythms of Neural Activity in DH44+ PI Neurons

(A) DH44 expression was not significantly different between *iso31* and *Nf1*$^{P1/P2}$ mutants. The bar graph shows mean ± SEM. n = 5 for iso31, and n = 6 for *Nf1*$^{P1/P2}$.

(B) Normalized fluorescence from calcium-dependent GFP expression in DH44-GAL4 > CaLexA/RedStinger flies. The complete genotypes are as follows: control: *UAS-RedStinger, lexAop2-mCD8::GFP/DH44-G4; UAS-mLEXA-VP16-NFAT, LexAop-CD2-GFP/+*. *Nf1*$^{P1/P2}$: *UAS-RedStinger, lexAop2-mCD8::GFP/DH44-G4; UAS-mLEXA-VP16-NFAT, LexAop-CD2-GFP, Nf1*^{P1}*/Nf1*^{P2}. Although CaLexA GFP signals in DH44 neurons were not significantly different between control and *Nf1*$^{P1/P2}$ flies at either the ZT1 or the ZT13 time point, there was a significant difference in fluorescence intensity between ZT1 and ZT13 in control flies (****p < 0.0001) that was not observed in *Nf1*$^{P1/P2}$ flies (one-way ANOVA and Tukey's multiple comparison test). n = 24–42 cells.

(C) Expression of transgenic *Nf1* in DH44 cells of *Nf1* mutant flies rescues cycling of calcium. Fluorescence from the CaLexA reporter in DH44 cells was normalized to the mean background intensity of the brain in *Nf1* mutants expressing *Nf1* in DH44 cells (*UAS-RedStinger, lexAop2-mCD8::GFP/+; UAS-mLEXA-VP16-NFAT, LexAop-CD2-GFP, Nf1*^{P1}*/DH44-Gal4, UAS-Nf1, Nf1*^{P1}) and in controls that lacked UAS-*Nf1* (*UAS-RedStinger, lexAop2-mCD8::GFP/+; UAS-mLEXA-VP16-NFAT, LexAop-CD2-GFP, Nf1*^{P1}*/DH44-Gal4, Nf1*^{P1}). JTK_CYCLE indicated a rhythm in rescued flies. n = 15–26 cells from 4–7 brains per time point.

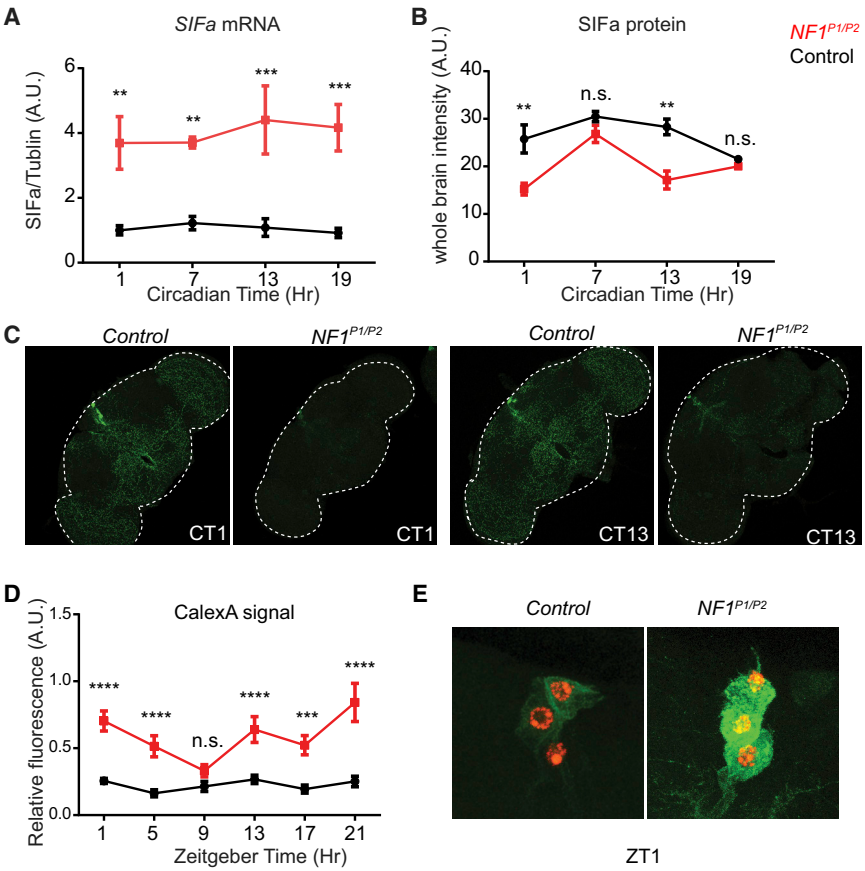

Figure 3. Expression of SIFa and Calcium Oscillations of SIFa+ PI Neurons Are Altered in $Nf1^{P1/P2}$ Mutant Flies

(A) *SIFa* mRNA levels throughout the day, normalized to α-tublin, in $Nf1^{P1/P2}$ mutants (red) and control iso31 (black) flies. Comparisons were with two-way ANOVA and Tukey post hoc test. **p < 0.01, ***p < 0.001. n = 5 independent experiments. Error bars represent SEM.

(B) SIFa staining intensity averaged over the whole brain in $Nf1^{P1/P2}$ mutants (red) and control *iso31* (black) flies. Comparisons were with two-way ANOVA and Tukey post hoc test. **p < 0.01, n.s., not significant. n = 36–48 cells each. Error bars represent SEM.

(C) Representative images of SIFa brain staining. The white dashed lines outline the brains.

(D) Normalized fluorescence from expression of the CaLexA reporter in SIFa neurons. The complete genotypes are as follows: control (black): *UAS-RedStinger, lexAop2-mCD8::GFP/SIFa-G4; UAS-mLEXA-VP16-NFAT/+*. $Nf1^{P1/P2}$ (red): *UAS-RedStinger, lexAop2-mCD8::GFP/SIFa-G4; UAS-mLEXA-VP16-NFAT,* $Nf1^{P1}/Nf1^{P2}$. Two-way ANOVA and Tukey's test. ***p < 0.001, ****p < 0.0001; n.s., not significant. n = 24–44 cells each. Error bars represent SEM.

(E) Representative images of the CaLexA GFP signal in SIFa neurons.

See also Figure S3.

rhythms of gene expression are assayed in such populations, but we were interested in this case in the levels of calcium over a 24-hr day. Astrocytes were treated with dexamethasone to synchronize circadian cycling, and calcium levels were assayed at different times of day with Cal-520, a recently developed fluorogenic calcium-sensitive dye (Lock et al., 2015) (Figure S4A). Whereas wild-type astrocytes displayed robust 24-hr oscillations of calcium (Figures 4A and 4B; Figure S3B), this cycling was dampened and the overall levels of calcium were higher in *Nf1*-deficient astrocytes (Figures 4C and 4D; Figure S4D). Altogether, these studies establish a conserved role for neurofibromin in regulating cellular activity rhythms within the nervous system.

DISCUSSION

Although the effects of neurofibromin on *Drosophila* circadian rhythms were reported more than 15 years ago, the cellular basis of action has remained elusive (Williams et al., 2001). Analysis of other circadian output molecules has also been difficult due to lack of a conceptual framework for output circuitry. Therefore, the identification of neurons downstream of the central clock (Cavanaugh et al., 2014) allows us to examine the function of output molecules in a cellular context. Leveraging these insights, we show that neurofibromin loss affects neural activity, as well as gene expression, in peptidergic neurons of a circadian circuit required for rest:activity rhythms. The demonstration that neurofibromin is similarly required for calcium-cellular activity rhythms in mouse astrocytes provides evidence for a conserved function of neurofibromin in the generation of rhythms.

Our findings suggest that neurofibromin acts broadly in the *Drosophila* circadian system. Multiple circadian neurons show cellular phenotypes in the *Nf1* mutant background, and only drivers with widespread expression rescue the mutant behavioral phenotype. In previous work, we found that clock function was normal in PDF cells, and neurofibromin expression in these cells was insufficient to drive rhythms (Williams et al., 2001; supported also by our current data). As a result, we did not examine the cycling of PDF at the dorsal termini of sLNvs. We now report that this cycling is altered, suggesting that *Nf1* affects outputs of the clock within PDF cells. The behavioral relevance of rhythmic PDF accumulation has been questioned (Kula et al., 2006), but subsequent studies have supported a role for cellular rhythms at LNv termini (Fernández et al., 2008; Helfrich-Förster et al., 2000). Loss of *Nf1* abrogates these cellular rhythms, in conjunction with loss of PDF cycling.

PDF expression at sLNv termini is also reduced, which is typically indicative of increased release (Kwon et al., 2015; Park et al., 2000) and consistent with increased MAPK activity in this region of the brain in *Nf1* mutants (Williams et al., 2001). Effects of *Nf1* mutants on rhythms are mediated through increased MAPK activity (Williams et al., 2001), which is also a

Table 3. *SIFa* Mutants Are Rhythmic

Genotype	N	SR (%)	MR (%)	WR (%)	AR (%)	FFT ± SEM	Period ± SEM (hr)
iso31	16	87.5	6.3	0.0	0.0	0.133 ± 0.016	23.83 ± 0.03
$SIFa^1$/+	11	100.0	0.0	0.0	0.0	0.140 ± 0.014	23.85 ± 0.05
$SIFa^1$	15	26.7	33.3	26.7	0.0	0.055 ± 0.011	24.04 ± 0.09
$SIFa^1$/Def	16	56.3	18.8	25.0	6.7	0.059 ± 0.011	24.59 ± 0.17
$SIFa^2$/+	8	100.0	0.0	0.0	0.0	0.149 ± 0.014	23.84 ± 0.08
$SIFa^2$	15	86.7	0.0	13.3	0.0	0.100 ± 0.013	23.89 ± 0.07
$SIFa^2$/Def	16	56.3	0.0	31.3	0.0	0.039 ± 0.005	24.14 ± 0.13
$SIFa^3$/+	5	100.0	0.0	0.0	0.0	0.120 ± 0.006	23.83 ± 0.03
$SIFa^3$	16	68.8	12.5	6.3	12.5	0.092 ± 0.013	23.94 ± 0.04
$SIFa^3$/Def	16	43.8	6.3	50.0	0.0	0.059 ± 0.010	24.86 ± 0.12

SR, strongly rhythmic; MR, moderately rhythmic; WR, weakly arrhythmic; AR, arrhythmic.

major target of neurofibromin in mammals (Rad and Tee, 2016). Conversely, *Pdf* mutants show decreased MAPK activity. In addition to affecting rhythmic outputs of the sLNvs, neurofibromin is implicated in signaling through the PDFR (Mertens et al., 2005). The impact of neurofibromin on PDF signaling is relevant to behavioral rhythms, because rhythm phenotypes of *pdfr* are partially rescued by a reduction in *Nf1* gene expression. We infer that increased PDF signaling caused by loss of one copy of *Nf1* compensates for reduced *pdfr* expression (*pdfr* mutants do not appear to be nulls) (Hyun et al., 2005; Lear et al., 2005; Mertens et al., 2005). *Nf1* mutants are not rescued by a reduction in *pdfr*, most likely because *Nf1* action at multiple sites contributes to the behavioral phenotype. Alternatively, lack of rescue may primarily reflect a need for neurofibromin action downstream of *pdfr*.

Clock function and neural activity are normal in DN1s of *Nf1* mutant flies. Although we cannot exclude other effects in DN1s—for instance, the increased MAPK activity mentioned earlier may occur in DN1s—it is unlikely that effects in DN1s account for the strong effect of *Nf1* on downstream PI cells. More likely, the PI phenotypes in *Nf1* mutant flies represent additional sites of neurofibromin action and are not secondary to upstream defects in the pathway. This interpretation is supported by cell-autonomous rescue of the phenotype in DH44 cells. It is also consistent with the broad requirement for neurofibromin in the rescue of behavioral rhythms and the lack of rescue of the *Nf1* behavioral phenotype by *pdfr* mutants.

Dampened cycling of neural activity in DH44 cells of the PI is likely an important contributor to the arrhythmic phenotype, because these cells are critical for circadian behavioral rhythms (Cavanaugh et al., 2014; King et al., 2017). The phase of calcium we report here is the same as that reported previously (Cavey et al., 2016) and consistent with a role for DH44 in the evening peak of locomotor activity (King et al., 2017). An even stronger phenotype is observed in *Nf1* mutants in cells that produce SIFa. These cells show very high activity and higher levels of SIFa mRNA, although the levels of protein are not elevated. We suggest that the protein does not accumulate because it is constantly secreted in response to the high neural activity; mRNA levels may increase to compensate for the continually depleted protein. *Nf1* phenotypes in circadian cells indicate not only a cellular mechanism of action but also potential molecular targets (PDF and SIFa). Genetic interactions of *Nf1* with *pdfr* in the context of circadian rhythms and with *SIFa* in the regulation of sleep suggest that these molecular targets are relevant for behavior. We suggest that effects of neurofibromin loss on sleep result from dysregulated SIFa signaling. Effects of *Drosophila Nf1* on peptidergic signaling are supported by a former report showing rescue of synaptic growth phenotypes in *Nf1* flies by a mutation in a peptide receptor (Walker et al., 2013).

To extend our findings of aberrant calcium signals and neural activity in *Nf1* mutant flies to higher organisms, we sought to determine whether these phenotypes were conserved in mammals. Herein, we show that astrocytes display rhythmic calcium cycling, likely reflecting rhythmic cellular activity, and that these rhythms are attenuated in $Nf1^{-/-}$ cells. Increased excitability and secretion phenotypes were found in *Nf1*-deficient mouse cells (Hingtgen et al., 2006; Wang et al., 2005), and although the mechanisms are still unclear, they may involve post-translational modification of N-type calcium channels (Duan et al., 2014). Given that neurofibromin is a potent regulator of MAPK activity, phosphorylation is a candidate mechanism for such modifications. However, effects of *Nf1* on cellular activity or excitability have not been studied in the context of rhythms. In addition, as indicated earlier, assays of behavioral rhythms in *Nf1* mutant mice have been complicated by the lethality of the null mutant.

The extent of neurofibromin loss in *Nf1* patients tends to vary considerably. Homozygous *Nf1* loss in human brain neurons has not yet been reported, but studies have demonstrated that not all germline *NF1* gene mutations are equivalent, with some leading to dramatic reductions in neurofibromin expression (>80%) and others exhibiting more modest effects (Anastasaki et al., 2015). Recapitulating these mutational differences in mice produces variations in the penetrance and severity of phenotypes (Toonen et al., 2016), which is likely also the case in humans. It is possible that circadian rhythm abnormalities would only be observed in individuals with strong hypomorphic germline mutations in the *Nf1* gene. Nevertheless, deficits in sleep initiation and maintenance have been reported in children with neurofibromatosis (Johnson et al., 2005; Leschziner et al., 2013; Licis et al., 2013;

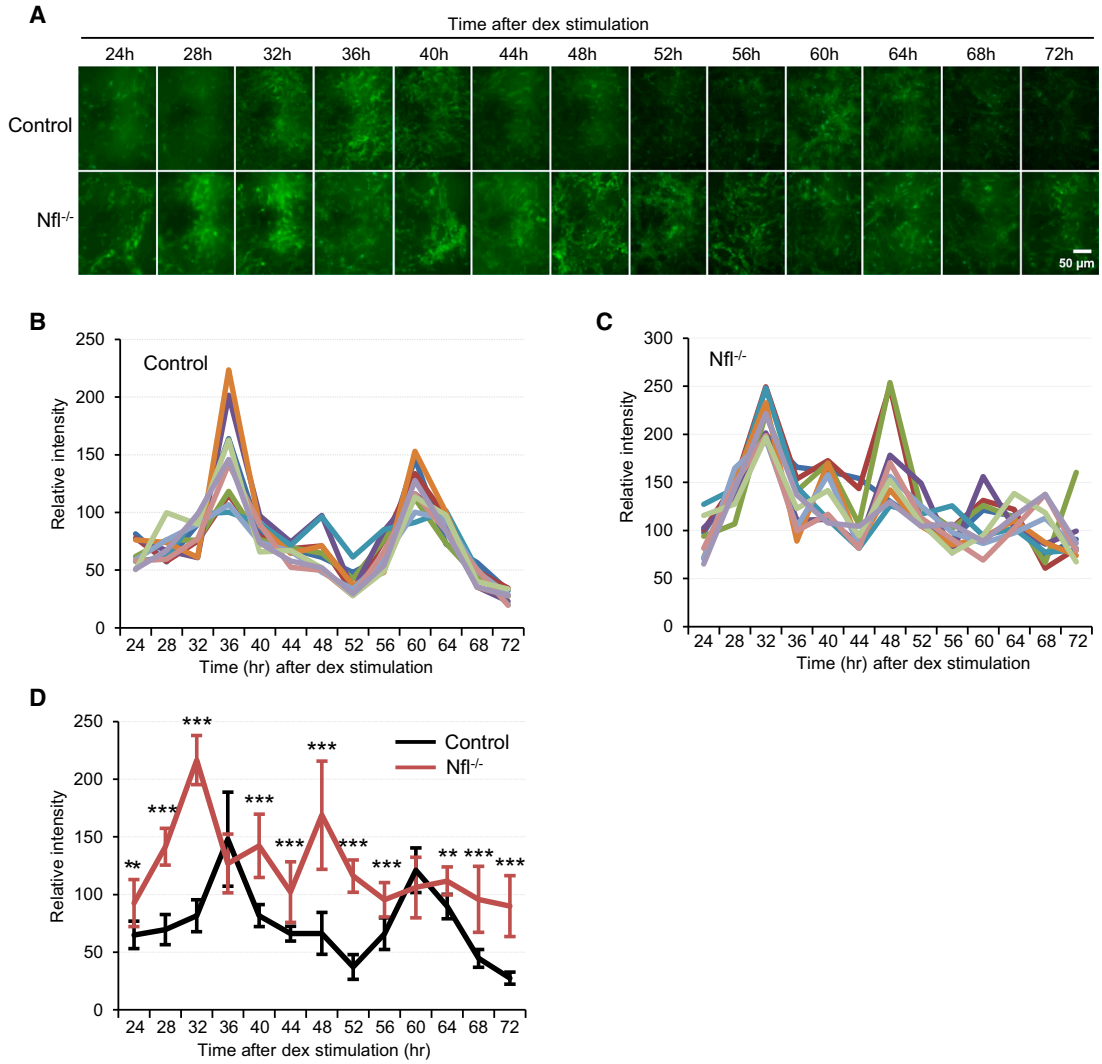

Figure 4. Genetic Ablation of *Nf1* Upregulates Calcium Levels and Disrupts Calcium Oscillations in Mammalian Astrocytes

(A) Fluorescence images of a time course of changes in calcium in wild-type (control) and *Nf1*$^{-/-}$ (MUT) astrocytes after dexamethasone stimulation. Images were taken at low magnification (40×) using a FITC filter set (474 nm excitation and 530 nm emission). Scale bar, 50 μm. See Figures S4A and S4B for detailed experimental procedures and higher-magnification images.

(B and C) Quantitative measurement of calcium changes in ten wild-type (control) astrocytes (B) or *Nf1*$^{-/-}$ (MUT) astrocytes (C) at the time points indicated. The results are plotted as line graphs. See Figure S4C for details of quantitative calcium measurements in single cells.

(D) Quantitative comparison of changes of calcium levels over time in wild-type (control) and mutant (MUT) astrocytes. Error bars represent SD of the mean. **$p < 0.05$, ***$p < 0.0005$.

Figure S4D provides statistical analysis of time-of-day effects, using JTK_CYCLE and Lomb-Scargle algorithms.

Maraña Pérez et al., 2015) and could have their basis in the mechanisms we report here.

EXPERIMENTAL PROCEDURES

Fly Lines

The GAL4 lines were used previously in the lab (Bai and Sehgal, 2015; Cavanaugh et al., 2014; Crocker et al., 2010). *Nf1*^{P1}, *Nf1*^{P2}, and UAS-*Nf1* lines were reported (Williams et al., 2001) and were outcrossed into an *iso31* background for 7 generations. Bloomington line Df27352 was used as an *SIFa* deficiency allele (2R:60C2;60D14) tested in transheterozygotes with *SIFa* CRISPR alleles. CaLexA flies were a gift from J. Wang. UAS-RedStinger flies were obtained from the Bloomington Drosophila Stock Center.

Generation of *Nsyb-GS* Flies

nsyb-GS construct was generated using Gateway cloning (Invitrogen) and the construct was targeted to the PhiC31-attP2 landing site on the third chromosome (3L:68A4) in *Drosophila*. A 1,917 bp fragment of the *Drosophila n-synaptobrevin* (Nsyb) promoter (matching the fragment used to generate *Nsyb-GAL4* flies by Julie Simpson, Janelia Farm Research Campus) was PCR amplified from *Canton-S* flies and recombined into the Gateway pDonr221 vector using primers containing Gateway attB1/2 sites: attB1_Nsyb1917_5′, 5′-GGGGACA

AGTTTGTACAAAAAAGCAGGCTgaattcgacctcaaagatggaagc-3′, and attB2_Nsyb1917_3′, 5′-GGGGACCACTTTGTACAAGAAAGCTGGGTAgaattcggctgtcgatgattagg-3′. The *Geneswitch* transgene was PCR amplified from *Elav-GS* flies (Osterwalder et al., 2001) and recombined into the Gateway pDonrP2rP3 vector using primers containing a 5′ Kozac sequence and Gateway attB2r/3 sites: attB2r_GS_5′, 5′-GGGGACAGCTTTCTTGTACAAAGTGGAAcaacatggactcccagcagccaga-3′, and attB3_GS_3′, 5′-GGGGACAACTTTGTATAATAAAGTTGCttaggagctgatctgactcagcaggg-3′. Entry vector insertions were verified by sequencing. The *Nsyb* promoter sequence was largely similar, but not identical, to sequences in FlyBase (4 mismatches). *Nsyb*-promoter and *Geneswitch* entry vectors were recombined into the *Drosophila* pBPGUw-R1R3-p10 vector (Haynes et al., 2015) and injected into flies. To verify induction of UAS expression with RU-486, *Nsyb-GS* flies were crossed to *UAS-mCD8-GFP* and brain-GFP expression was compared in flies fed with or without 500 μM RU-486 (Mifepristone, Sigma) in the food. Although a low level of GFP expression was apparent in flies without RU-486, indicating some leakiness, GFP intensity was dramatically brighter in flies fed RU-486.

Generation of *SIFa* Mutants

The *SIFa* mutants were generated with CRISPR/Cas9-mediated genome editing (Port et al., 2014). Tandem *SIFa*-targeting guide RNA sequences flanking the *SIFa* coding region were introduced into pCFD4 (Addgene plasmid 49411) using the primers *SIFa*-KO-Forward (5′-TATATAGGAAAGATATCCGGGTGAACTTCGTAggctcgagatcagttctGTTTTAGAGCTAGAAATAGCAAG-3′) and SIFa-KO-Reverse (5′-ATTTTAACTTGCTATTTCTAGCTCTAAAACcaacgctcaccgaaaactgcGACGTTAAATTGAAAATAGGTC-3′) (*SIFa*-specific sequences are in lowercase) and following the protocol as described in http://www.crisprflydesign.org/wp-content/uploads/2014/06/Cloning-with-pCFD4.pdf. The targeting plasmid was injected into fly embryos (Bloomington Drosophila Stock Center [BDSC] 51323) using BestGene Transgenic services. We screened for deletions in the *SIFa* gene region with PCR sequencing using the primers *SIFa*_del_F1 (5′-aagcaggagagcgagttcag-3′) and *SIFa*_del_R1 (5′-ttcgccttgttttgtcacag-3′). Three *SIFa* deletion lines with minor differences in the *SIFa* genomic region were characterized ($SIFa^1$ deletion 2R:24577800-24578100, $SIFa^2$ deletion 2R:24577763-24578080, and $SIFa^3$ deletion 2R:24577787-24578087). All three deletions cover both exons of *SIFa*. The mutant lines were backcrossed to iso31 flies 7 times before testing.

Immunohistochemistry

Adult fly brains were dissected in cold PBS with 0.1% Triton-X (PBST) and fixed in 4% formaldehyde for 15–20 min on ice. Brains were rinsed 3 × 10 min with PBST, blocked for 30–60 min in 5% normal donkey serum in PBST (NDST), and incubated overnight (ON) at 4°C in primary antibody diluted in NDST. Brains were then rinsed 4 × 10 min in PBST, incubated 2 hr in secondary antibody diluted in NDST, rinsed 4 × 10 min in PBST, and mounted with Vectashield. The following primary antibodies were used: rabbit anti-GFP 1:1,000 (Molecular Probes A-11122), rabbit anti-DH44 1:500 (Johnson et al., 2005), guinea pig anti-PER 1:1,000 (I. Edery), mouse anti-PDF 1:500 (Developmental Studies Hybridoma Bank PDFC7; generated by J. Blau), and rabbit anti-SIFa 1:4,000 (gift from J. Veenstra). Secondary antibodies were as follows: Alexa Fluor 488 goat anti-rabbit 1:500 (Molecular Probes A-11008), fluorescein isothiocyanate (FITC) anti-guinea pig 1:500 (Jackson Laboratory 106-095-003), Cy5 donkey anti-mouse 1:400 (Jackson Laboratory 715-175-151), and Alexa Fluor 633 goat anti-rabbit (Molecular Probes A-21070). GFP signal from the CaLexA reporter system was detected with rabbit anti-GFP antibody followed by Alexa Fluor 488 goat anti-rabbit secondary antibody. Immunolabeled brains were visualized with a TCS SP5 confocal microscope.

Image Analysis

All images were analyzed with ImageJ software. For PDF intensity at sLNv dorsal termini, the terminus region was manually selected as a box, including the axon terminus upward from the branching point, and then thresholded with the average background staining level for the boxed region. The integrated intensity was measured and compared between genotypes. For quantification of CaLexA signals, each cytoplasmic area was manually selected and mean intensity was measured. Nuclear RedStinger expression is calcium independent and was used to normalize the GFP signals, except in Figure 2C, where the GFP signals were normalized to the mean background intensity of the brain.

Sleep Assays

Sleep was monitored with the single-beam Drosophila Activity Monitoring System (Trikinetics, Waltham, MA) or, when indicated, with multi-beam monitors (Trikinetics, Waltham, MA) as described previously (Bai and Sehgal, 2015).

Rest:Activity Rhythm Analysis

Locomotor activity assays were performed with the Drosophila Activity Monitoring System (Trikinetics, MA) as described previously (Cavanaugh et al., 2014). Individual male flies were loaded into glass tubes containing 5% sucrose and 2% agar. Flies were entrained to a 12:12 light:dark (LD) cycle for 3 days and then transferred to constant darkness. Locomotor activity during days 1–7 in constant darkness was analyzed with Clocklab software (Actimetrics, Wilmette, IL). A fly was considered rhythmic if it met 2 criteria: it displayed (1) a rhythm with 95% confidence using $\chi 2$ periodogram analysis and (2) a corresponding fast Fourier transform (FFT) value above 0.01 for the determined period. Rhythm strength was categorized as weak (0.01–0.03), moderate (0.03–0.05), or strong ($\geq$0.05).

Rhythms in Astrocyte Cultures

Wild-type and $Nf1^{-/-}$ astrocyte cultures were generated as previously described (Smithson and Gutmann, 2016). Brainstem astrocytes obtained from $Nf1^{flox/flox}$ mouse pups (postnatal days 1–2) were infected with adenovirus type 5 containing β-galactosidase (Ad5-LacZ) or Cre recombinase (Ad5-Cre) (University of Iowa Gene Transfer Core, Iowa City, IA) to produce wild-type or $Nf1^{-/-}$ astrocytes, respectively. Loss of neurofibromin expression was confirmed by western blotting (Santa Cruz sc-67).

Following three passages (including those in which cells were generated and manipulated to delete *Nf1*), wild-type and $Nf1^{-/-}$ astrocytes were seeded overnight at 50,000 cells per well in 24 wells with collagen-coated coverslips. 24 hr after treatment with 1 μM dexamethasone (Sigma D2915), 4 μM Cal 520 acetoxymethyl ester (AM) (Abcam ab171868) in Hank's balanced salt solution (HBSS; Thermo Fisher Scientific 14175079) buffer with 1 mM probenecid (Abcam ab145725) was added into the wells at the indicated time points, and the cells were incubated at 37°C for 2 hr. The addition of probenecid inhibited organic anion transporters and thereby reduce efflux of the calcium indicator from the cell. The cells were washed three times with HBSS containing 1 mM probenecid and then fixed with 4% paraformaldehyde (PFA). They were imaged with a fluorescence microscope using FITC (excitation [Ex.] = 492 nm and emission [Em.] = 514 nm) and DAPI (Ex. = 370 nm and Em. = 460 nm) filter sets with the same light exposure time. For statistical analysis, the fluorescence intensity of ten wild-type or mutant cells was measured at each time point using ImageJ analysis software, and the results were plotted as line graphs. For statistical analyses of circadian parameters, the calcium data were subjected to Jonckheere-Terpstra-Kendall (JTK)_CYCLE and Lomb-Scargle (LS) analysis using the Meta-cycle R program as described (Wu et al., 2016).

Statistics

Data were analyzed and plotted with the GraphPad Prism software. Details of statistical analysis are provided in the figure legends, along with the p values corresponding to the asterisks in the figures.

SUPPLEMENTAL INFORMATION

Supplemental Information includes four figures and can be found with this article online at https://doi.org/10.1016/j.celrep.2018.03.014.

ACKNOWLEDGMENTS

We thank Laura J. Smithson for the astrocyte cultures, Nicholas Lahens for help with statistical analysis, and members of the Sehgal laboratory for helpful discussions over the course of this project. The work was supported by R37-NS-048471 to A.S. D.H.G. is supported by a Research Program Award

from the National Institute of Neurological Disorders and Stroke (1-R35-NS097211-01).

AUTHOR CONTRIBUTIONS

Conceptualization, L.B., X.Z., and A.S.; Methodology: L.B., Y.L., D.C., and D.H.G.; Investigation, L.B., Y.L., C.T.H., J.A.W., D.C., X.Z., and H.W.; Resources, C.S., P.H., and D.H.G.; Writing – Original Draft, L.B. and A.S.; Writing – Reviewing & Editing, A.S., L.B., D.H.G., J.A.W., and Y.L.; Funding Acquisition, A.S. and D.H.G.; Supervision, A.S.

DECLARATION OF INTERESTS

The authors declare no competing interests.

Received: August 4, 2017
Revised: December 21, 2017
Accepted: March 2, 2018
Published: March 27, 2018

REFERENCES

Anastasaki, C., Woo, A.S., Messiaen, L.M., and Gutmann, D.H. (2015). Elucidating the impact of neurofibromatosis-1 germline mutations on neurofibromin function and dopamine-based learning. Hum. Mol. Genet. *24*, 3518–3528.

Artiushin, G., and Sehgal, A. (2017). The *Drosophila* circuitry of sleep-wake regulation. Curr. Opin. Neurobiol. *44*, 243–250.

Bai, L., and Sehgal, A. (2015). anaplastic lymphoma kinase acts in the *Drosophila* mushroom body to negatively regulate sleep. PLoS Genet. *11*, e1005611.

Balsalobre, A., Brown, S.A., Marcacci, L., Tronche, F., Kellendonk, C., Reichardt, H.M., Schütz, G., and Schibler, U. (2000). Resetting of circadian time in peripheral tissues by glucocorticoid signaling. Science *289*, 2344–2347.

Barber, A.F., Erion, R., Holmes, T.C., and Sehgal, A. (2016). Circadian and feeding cues integrate to drive rhythms of physiology in *Drosophila* insulin-producing cells. Genes Dev. *30*, 2596–2606.

Barca-Mayo, O., Pons-Espinal, M., Follert, P., Armirotti, A., Berdondini, L., and De Pietri Tonelli, D. (2017). Astrocyte deletion of Bmal1 alters daily locomotor activity and cognitive functions via GABA signalling. Nat. Commun. *8*, 14336.

Brancaccio, M., Patton, A.P., Chesham, J.E., Maywood, E.S., and Hastings, M.H. (2017). Astrocytes control circadian timekeeping in the suprachiasmatic nucleus via glutamatergic signaling. Neuron *93*, 1420–1435.

Buchanan, M.E., and Davis, R.L. (2010). A distinct set of *Drosophila* brain neurons required for neurofibromatosis type 1-dependent learning and memory. J. Neurosci. *30*, 10135–10143.

Cavanaugh, D.J., Geratowski, J.D., Wooltorton, J.R., Spaethling, J.M., Hector, C.E., Zheng, X., Johnson, E.C., Eberwine, J.H., and Sehgal, A. (2014). Identification of a circadian output circuit for rest:activity rhythms in *Drosophila*. Cell *157*, 689–701.

Cavey, M., Collins, B., Bertet, C., and Blau, J. (2016). Circadian rhythms in neuronal activity propagate through output circuits. Nat. Neurosci. *19*, 587–595.

Crocker, A., Shahidullah, M., Levitan, I.B., and Sehgal, A. (2010). Identification of a neural circuit that underlies the effects of octopamine on sleep:wake behavior. Neuron *65*, 670–681.

Duan, J.H., Hodgdon, K.E., Hingtgen, C.M., and Nicol, G.D. (2014). N-type calcium current, Cav2.2, is enhanced in small-diameter sensory neurons isolated from Nf1+/− mice. Neuroscience *270*, 192–202.

Fernández, M.P., Berni, J., and Ceriani, M.F. (2008). Circadian remodeling of neuronal circuits involved in rhythmic behavior. PLoS Biol. *6*, e69.

Gorczyca, M.G., and Hall, J.C. (1987). Immunohistochemical localization of choline acetyltransferase during development and in Chats mutants of *Drosophila melanogaster*. J. Neurosci. *7*, 1361–1369.

Guo, F., Yu, J., Jung, H.J., Abruzzi, K.C., Luo, W., Griffith, L.C., and Rosbash, M. (2016). Circadian neuron feedback controls the *Drosophila* sleep-activity profile. Nature *536*, 292–297.

Haynes, P.R., Christmann, B.L., and Griffith, L.C. (2015). A single pair of neurons links sleep to memory consolidation in *Drosophila melanogaster*. eLife *4*, e03868.

Helfrich-Förster, C., Täuber, M., Park, J.H., Mühlig-Versen, M., Schneuwly, S., and Hofbauer, A. (2000). Ectopic expression of the neuropeptide pigment-dispersing factor alters behavioral rhythms in *Drosophila melanogaster*. J. Neurosci. *20*, 3339–3353.

Hewes, R.S., Schaefer, A.M., and Taghert, P.H. (2000). The cryptocephal gene (ATF4) encodes multiple basic-leucine zipper proteins controlling molting and metamorphosis in *Drosophila*. Genetics *155*, 1711–1723.

Hingtgen, C.M., Roy, S.L., and Clapp, D.W. (2006). Stimulus-evoked release of neuropeptides is enhanced in sensory neurons from mice with a heterozygous mutation of the Nf1 gene. Neuroscience *137*, 637–645.

Hyun, S., Lee, Y., Hong, S.T., Bang, S., Paik, D., Kang, J., Shin, J., Lee, J., Jeon, K., Hwang, S., et al. (2005). *Drosophila* GPCR Han is a receptor for the circadian clock neuropeptide PDF. Neuron *48*, 267–278.

Im, S.H., and Taghert, P.H. (2010). PDF receptor expression reveals direct interactions between circadian oscillators in *Drosophila*. J. Comp. Neurol. *518*, 1925–1945.

Johnson, H., Wiggs, L., Stores, G., and Huson, S.M. (2005). Psychological disturbance and sleep disorders in children with neurofibromatosis type 1. Dev. Med. Child Neurol. *47*, 237–242.

King, A.N., Barber, A.F., Smith, A.E., Dreyer, A.P., Sitaraman, D., Nitabach, M.N., Cavanaugh, D.J., and Sehgal, A. (2017). A peptidergic circuit links the circadian clock to locomotor activity. Curr. Biol. *27*, 1915–1927.

Kula, E., Levitan, E.S., Pyza, E., and Rosbash, M. (2006). PDF cycling in the dorsal protocerebrum of the *Drosophila* brain is not necessary for circadian clock function. J. Biol. Rhythms *21*, 104–117.

Kwon, Y., Song, W., Droujinine, I.A., Hu, Y., Asara, J.M., and Perrimon, N. (2015). Systemic organ wasting induced by localized expression of the secreted insulin/IGF antagonist ImpL2. Dev. Cell *33*, 36–46.

Lakkis, M.M., Golden, J.A., O'Shea, K.S., and Epstein, J.A. (1999). Neurofibromin deficiency in mice causes exencephaly and is a modifier for Splotch neural tube defects. Dev. Biol. *212*, 80–92.

Lear, B.C., Merrill, C.E., Lin, J.M., Schroeder, A., Zhang, L., and Allada, R. (2005). A G protein-coupled receptor, groom-of-PDF, is required for PDF neuron action in circadian behavior. Neuron *48*, 221–227.

Leschziner, G.D., Golding, J.F., and Ferner, R.E. (2013). Sleep disturbance as part of the neurofibromatosis type 1 phenotype in adults. Am. J. Med. Genet. A. *161A*, 1319–1322.

Licis, A.K., Vallorani, A., Gao, F., Chen, C., Lenox, J., Yamada, K.A., Duntley, S.P., and Gutmann, D.H. (2013). Prevalence of sleep disturbances in children with neurofibromatosis type 1. J. Child Neurol. *28*, 1400–1405.

Lock, J.T., Parker, I., and Smith, I.F. (2015). A comparison of fluorescent Ca^{2+} indicators for imaging local Ca^{2+} signals in cultured cells. Cell Calcium *58*, 638–648.

Maraña Pérez, A.I., Duat Rodríguez, A., Soto Insuga, V., Domínguez Carral, J., Puertas Martín, V., and González Gutiérrez Solana, L. (2015). Prevalence of sleep disorders in patients with neurofibromatosis type 1. Neurologia *30*, 561–565.

Masuyama, K., Zhang, Y., Rao, Y., and Wang, J.W. (2012). Mapping neural circuits with activity-dependent nuclear import of a transcription factor. J. Neurogenet. *26*, 89–102.

Mertens, I., Vandingenen, A., Johnson, E.C., Shafer, O.T., Li, W., Trigg, J.S., De Loof, A., Schoofs, L., and Taghert, P.H. (2005). PDF receptor signaling in *Drosophila* contributes to both circadian and geotactic behaviors. Neuron *48*, 213–219.

Osterwalder, T., Yoon, K.S., White, B.H., and Keshishian, H. (2001). A conditional tissue-specific transgene expression system using inducible GAL4. Proc. Natl. Acad. Sci. USA *98*, 12596–12601.

Park, J.H., Helfrich-Förster, C., Lee, G., Liu, L., Rosbash, M., and Hall, J.C. (2000). Differential regulation of circadian pacemaker output by separate clock genes in *Drosophila*. Proc. Natl. Acad. Sci. USA *97*, 3608–3613.

Park, S., Sonn, J.Y., Oh, Y., Lim, C., and Choe, J. (2014). SIFamide and SIFamide receptor defines a novel neuropeptide signaling to promote sleep in *Drosophila*. Mol. Cells *37*, 295–301.

Port, F., Chen, H.M., Lee, T., and Bullock, S.L. (2014). Optimized CRISPR/Cas tools for efficient germline and somatic genome engineering in *Drosophila*. Proc. Natl. Acad. Sci. USA *111*, E2967–E2976.

Rad, E., and Tee, A.R. (2016). Neurofibromatosis type 1: Fundamental insights into cell signalling and cancer. Semin. Cell Dev. Biol. *52*, 39–46.

Smithson, L.J., and Gutmann, D.H. (2016). Proteomic analysis reveals GIT1 as a novel mTOR complex component critical for mediating astrocyte survival. Genes Dev. *30*, 1383–1388.

Toonen, J.A., Anastasaki, C., Smithson, L.J., Gianino, S.M., Li, K., Kesterson, R.A., and Gutmann, D.H. (2016). NF1 germline mutation differentially dictates optic glioma formation and growth in neurofibromatosis-1. Hum. Mol. Genet. *25*, 1703–1713.

Tso, C.F., Simon, T., Greenlaw, A.C., Puri, T., Mieda, M., and Herzog, E.D. (2017). Astrocytes regulate daily rhythms in the suprachiasmatic nucleus and behavior. Curr. Biol. *27*, 1055–1061.

Walker, J.A., Gouzi, J.Y., Long, J.B., Huang, S., Maher, R.C., Xia, H., Khalil, K., Ray, A., Van Vactor, D., Bernards, R., and Bernards, A. (2013). Genetic and functional studies implicate synaptic overgrowth and ring gland cAMP/PKA signaling defects in the *Drosophila melanogaster* neurofibromatosis-1 growth deficiency. PLoS Genet. *9*, e1003958.

Wang, Y., Nicol, G.D., Clapp, D.W., and Hingtgen, C.M. (2005). Sensory neurons from Nf1 haploinsufficient mice exhibit increased excitability. J. Neurophysiol. *94*, 3670–3676.

Weiss, J.B., Weber, S.J., Torres, E.R.S., Marzulla, T., and Raber, J. (2017). Genetic inhibition of Anaplastic Lymphoma Kinase rescues cognitive impairments in Neurofibromatosis 1 mutant mice. Behav. Brain Res. *321*, 148–156.

Williams, J.A., Su, H.S., Bernards, A., Field, J., and Sehgal, A. (2001). A circadian output in *Drosophila* mediated by neurofibromatosis-1 and Ras/MAPK. Science *293*, 2251–2256.

Wu, G., Anafi, R.C., Hughes, M.E., Kornacker, K., and Hogenesch, J.B. (2016). MetaCycle: an integrated R package to evaluate periodicity in large scale data. Bioinformatics *32*, 3351–3353.

Cell Reports, Volume *22*

Supplemental Information

A Conserved Circadian Function for the *Neurofibromatosis 1* Gene

Lei Bai, Yool Lee, Cynthia T. Hsu, Julie A. Williams, Daniel Cavanaugh, Xiangzhong Zheng, Carly Stein, Paula Haynes, Han Wang, David H. Gutmann, and Amita Sehgal

A

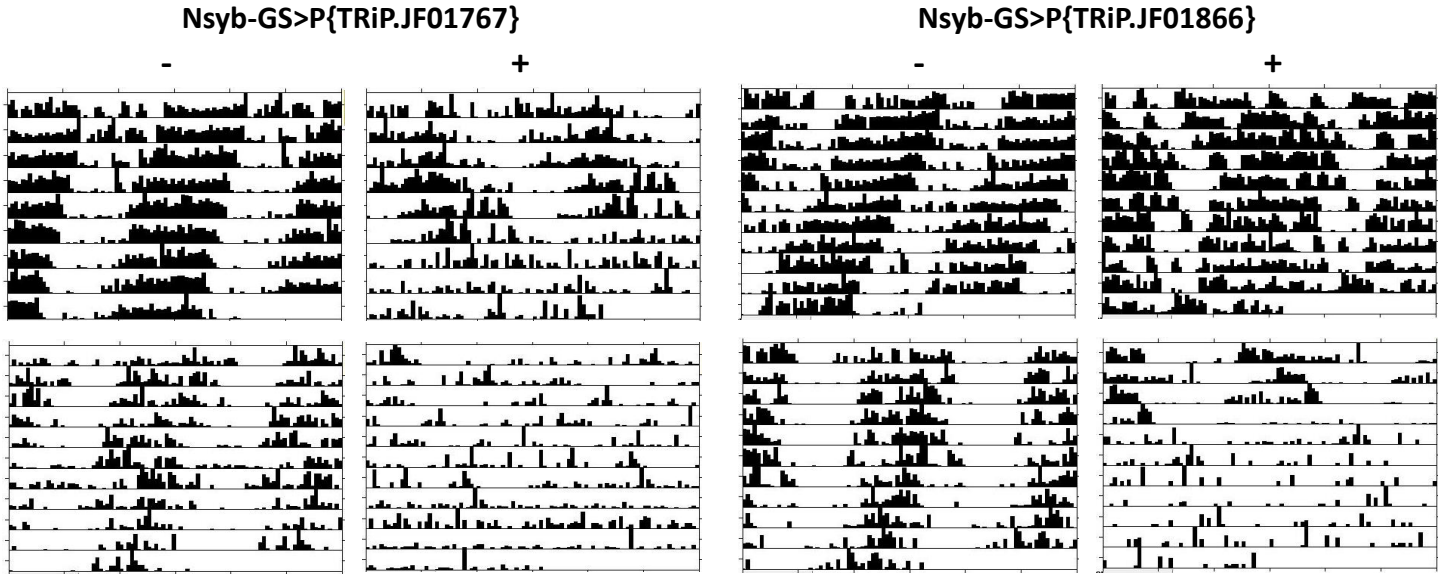

B

M/F	RU	#Rhythmic/N	X^2 Tau	Rel FFT Power
Nsyb-GS>P{TRiP.JF01767}				
M	-	31/31	22.92 ± 0.08	0.156 ± 0.01
	+	24/30	24.46 ± 0.16***	0.088 ± 0.01***
F	-	22/24	23.45 ± 0.15	0.097 ± 0.01
	+	11/20	23.13 ± 0.52	0.057 ± 0.01**
Nsyb-GS>P{TRiP.JF01866}				
M	-	28/28	23.16 ± 0.08	0.176 ± 0.01
	+	25/28	24.44 ± 0.13***	0.141 ± 0.01
F	-	24/24	23.75 ± 0.11	0.190 ± 0.01
	+	21/24	24.05 ± 0.54*	0.111 ± 0.01**
Nsyb-GS>+				
M	-	16/16	23.22 ± 0.14	0.187 ± 0.02
	+	14/14	25.11 ± 0.32***	0.166 ± 0.02
F	-	13/15	23.88 ± 0.10	0.091 ± 0.01
	+	13/14	25.35 ± 0.19***	0.147 ± 0.02*

Supplemental Figure 1 (Related to main Table 1). RNAi-mediated knockdown of *Nf1* with an inducible pan-neuronal driver (Nsyb-GS) alters circadian rhythms. **A**. Representative actograms of individual flies of indicated genotypes. Locomotor activity was recorded in constant darkness for 9-11 days as shown. Males fed vehicle (-) or RU-486 (+) are shown in the top panels and females are in the lower panels. **B**. Period length as measured by Chi^2 and relative FFT power are reported for males and females of indicated RNAi lines with (+) and without (-) RU-486. Comparisons were between (+) and (-) groups; * =p< 0.05, ** = p<0.009, and *** =p<0.0001, student's t-test.

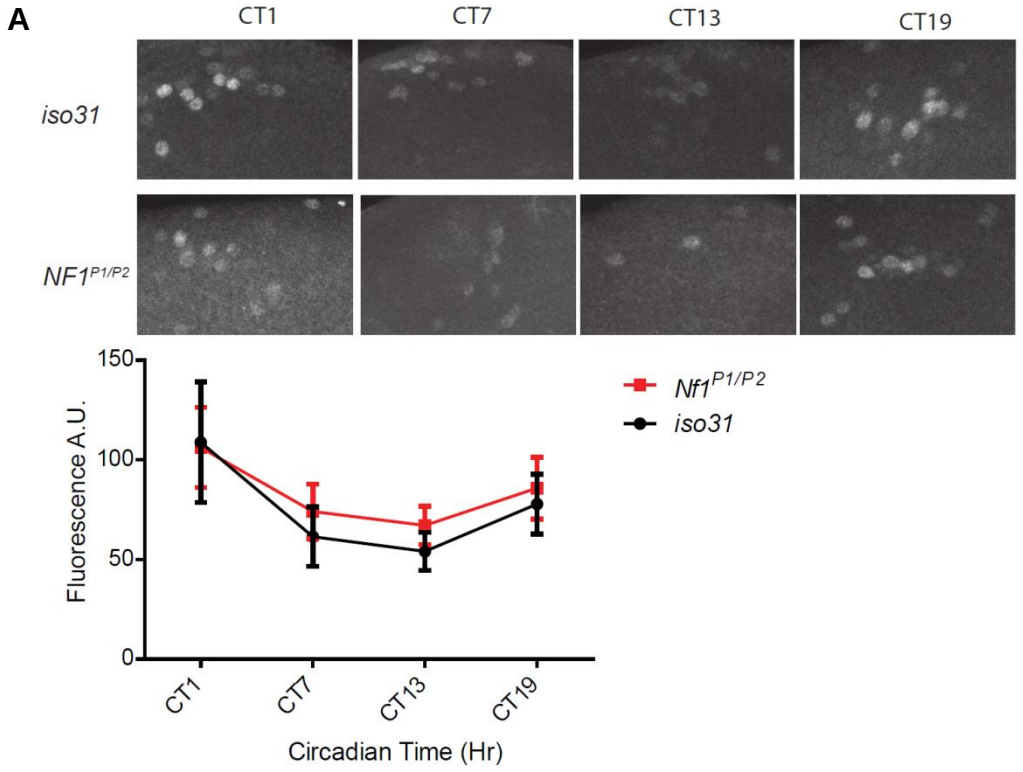
A
CT1
CT7
CT13
CT19
iso31
NF1P1/P2
150
100
50
0
Fluorescence A.U.
Nf1P1/P2
iso31
CT1
CT7
CT13
CT19
Circadian Time (Hr)

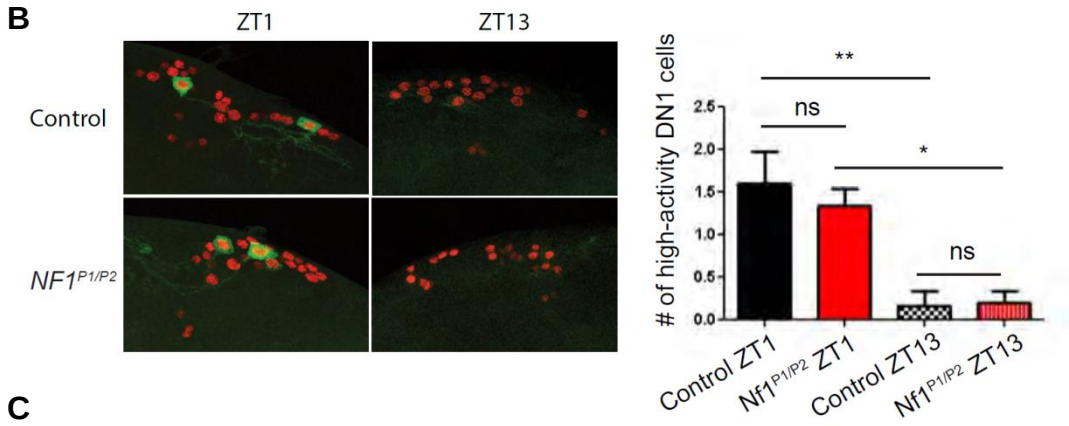
B
ZT1
ZT13
Control
NF1P1/P2
**
ns
*
ns
# of high-activity DN1 cells
2.5
2.0
1.5
1.0
0.5
0.0
Control ZT1
Nf1P1/P2 ZT1
Control ZT13
Nf1P1/P2 ZT13

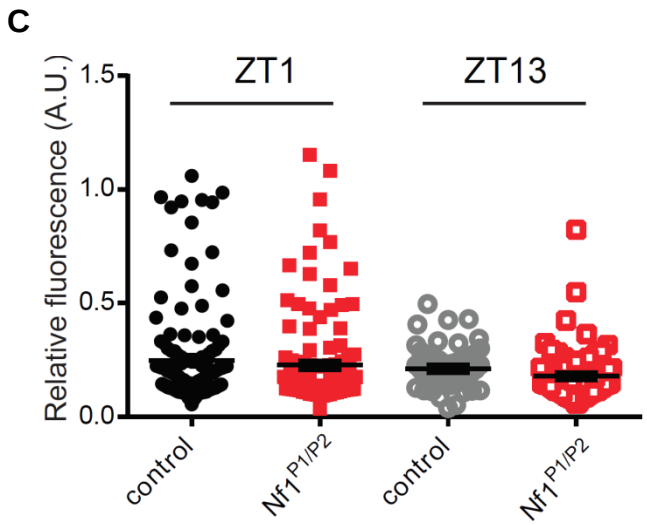
C
ZT1
ZT13
Relative fluorescence (A.U.)
1.5
1.0
0.5
0.0
control
Nf1P1/P2
control
Nf1P1/P2

Supplemental Figure 2 (Related to main Figure 1). DN1 clock cells display normal molecular cycling and activity patterns in *Nf1* mutant flies. (A) PER protein staining in the DN1 neurons in constant darkness. Representative images of 7-8 brains per time point are shown in the top panel. Average DN1 fluorescence intensity per brain was plotted as mean±SEM. *Iso31* and $Nf1^{P1/P2}$ were not significantly different at any time point (One-way ANOVA and Tukey's multiple comparison tests). (B) Calcium-dependent GFP expression in InSITE 911-GAL4>UAS-CaLexA/UAS-RedStinger flies. All DN1 neurons were labeled with nuclear RedStinger. Images are representative of 8-12 brains. The number of DN1 cells with high fluorescence (normalized to the RedStinger signal, ≥0.50) was significantly higher at ZT1 than at ZT13 in both control and $Nf1^{P1/P2}$ flies (One-way ANOVA and Tukey's tests). Bar graph shows mean and SEM. N=8-12 brains. (C) Quantification of calcium-dependent GFP expression in all DN1 cells detected in wild type and mutant flies at ZT 1. Normalized GFP intensity was determined for individual DN1 neurons. Lines and error bars are mean and SEM, respectively. One-way ANOVA and Tukey's multiple comparison test did not detect any difference between control and $Nf1^{P1/P2}$ at either time point, when fluorescence in all DN1s was taken into account. Thus, DN1s are similar at ZT1 and ZT13 in terms of overall calcium signal, but the number of DN1s with high calcium-dependent fluorescence (≥ 0.50) is greater at ZT1 (shown in B) in both control and $Nf1^{P1/P2}$ flies.

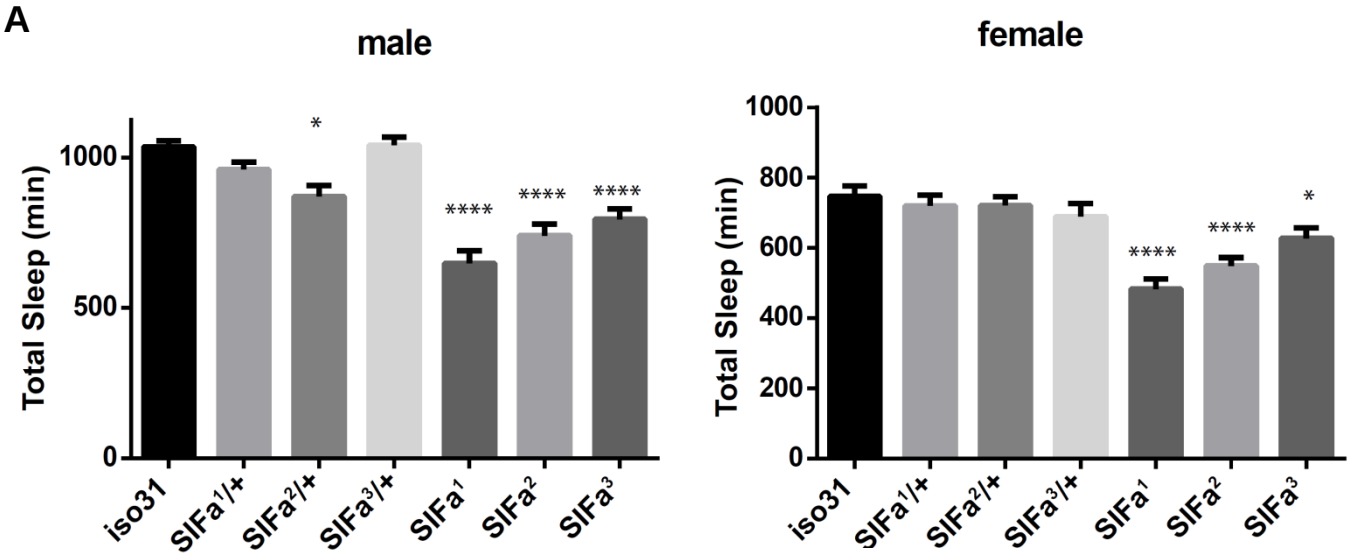
A
male
female
Total Sleep (min)
1000
500
0
1000
800
600
400
200
0
*
****
****
****
****
*
iso31
SIFa1/+
SIFa2/+
SIFa3/+
SIFa1
SIFa2
SIFa3

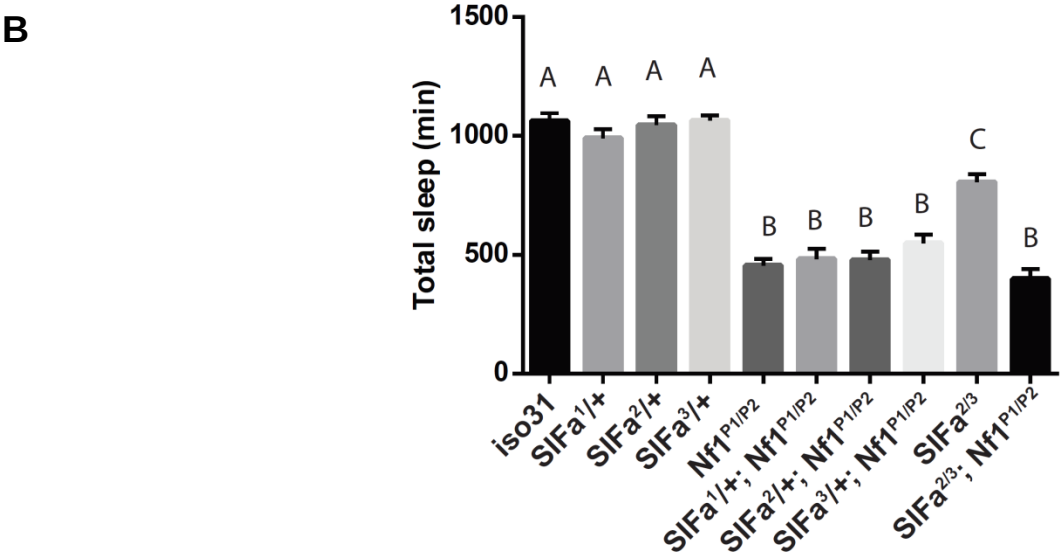
B
Total sleep (min)
1500
1000
500
0
A
A
A
A
B
B
B
B
C
B
iso31
SIFa1/+
SIFa2/+
SIFa3/+
Nf1P1/P2
SIFa1/+; Nf1P1/P2
SIFa2/+; Nf1P1/P2
SIFa3/+; Nf1P1/P2
SIFa2/3
SIFa2/3; Nf1P1/P2

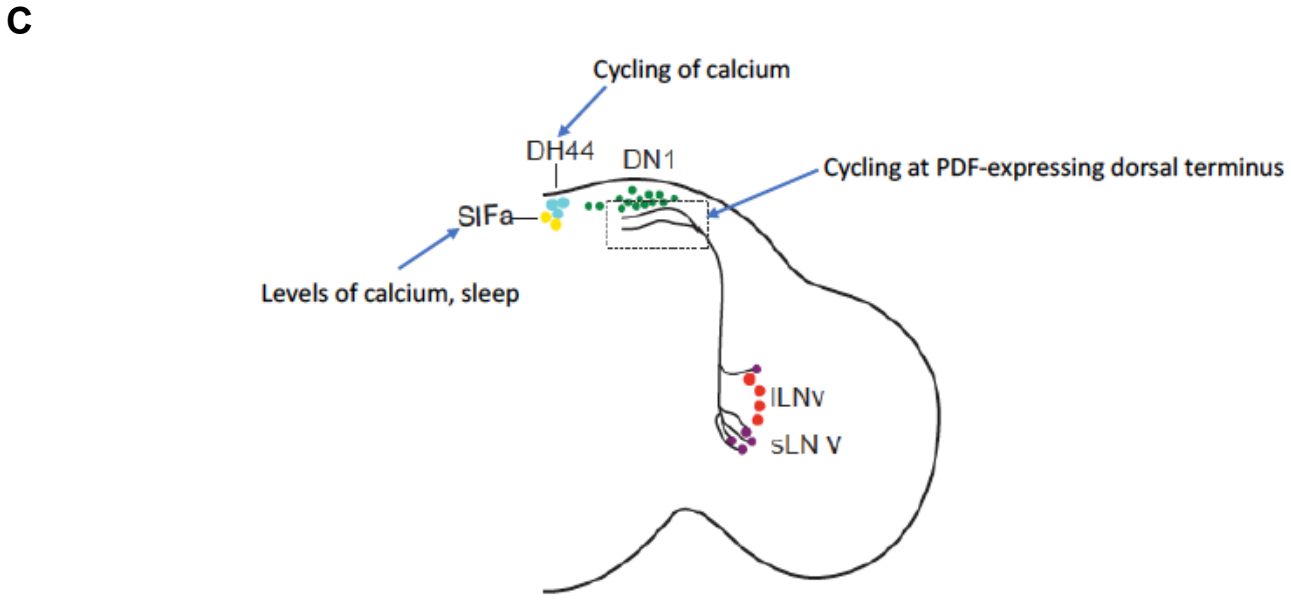
C
Cycling of calcium
DH44
DN1
Cycling at PDF-expressing dorsal terminus
SIFa
Levels of calcium, sleep
lLNv
sLN v

Supplemental Figure 3 (Related to main Figure 3). *SIFa* mutants have reduced sleep. (A) Total sleep is shown for males and females (mean±SEM) in wildtype control, SIFa heterozygous and SIFa homozygous fly lines. N=5-16 for males and 12-16 for females. Significant differences were found with one-way ANOVA analysis and Tukey's multiple comparison tests. *indicates significant difference from control iso31 flies. *P<0.05; ****P<0.0001. (B) Data for double mutants of SIFamide and *Nf1* are shown. *Nf1* is epistatic to *SIFa* in the regulation of sleep. Total sleep measured with multi-beam monitors is shown as mean±SEM. Groups with the same alphabetic label on top are not statistically different from each other; groups with different labels are statistically different (P<0.05). While both $SIFa^{2/3}$ and $Nf1^{P1/P2}$ mutants have reduced sleep compared to iso31, $SIFa^{2/3}$; $Nf1^{P1/P2}$ double mutants do not show a further sleep decrease relative to $Nf1^{P1/P2}$.flies. N=8-16. (C) Schematic representation of *Nf1* function in the circadian circuit. The cellular phenotype observed in each cell type is indicated. As *SIFa* and *Nf1* may affect sleep through the same pathway, sleep is noted as a possible phenotype associated with *SIFa* cells.

A

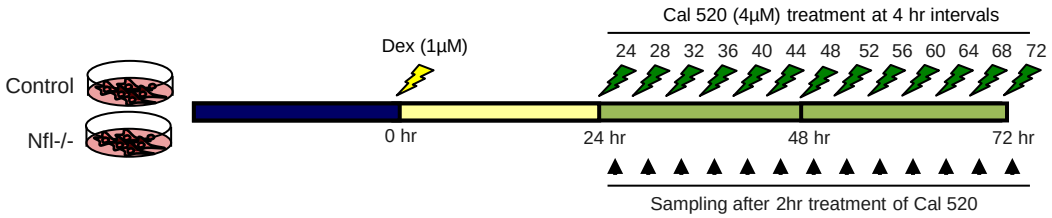

B

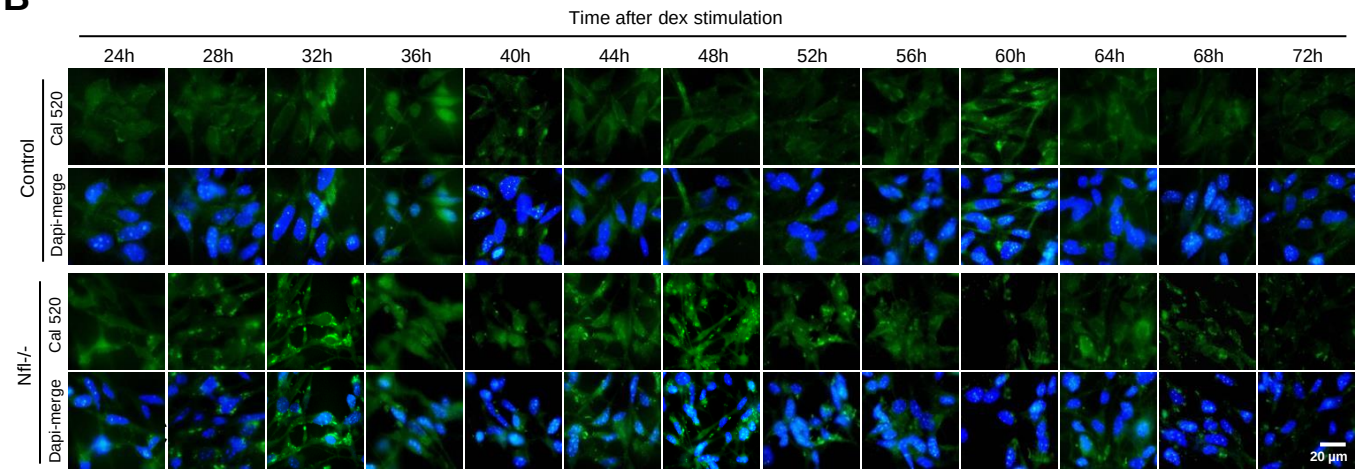

C

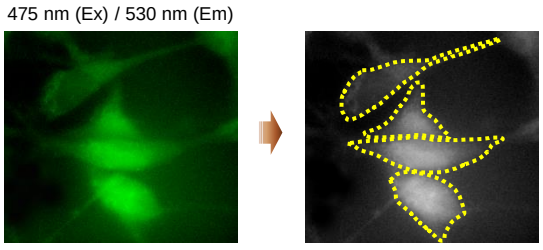

D

JTK cycle analysis results

CycID	BH.Q	P	Period	Phase	Amplitude
Control	1.07E-20	5.36E-21	24	14	24.1399184
Nfl-/-	0.01945527	0.01945527	24	8	8.650744361

LS analysis results

CycID	BH.Q	P	Period	Phase
Control	2.60E-12	1.30E-12	24.0	36.3
Nfl-/-	0.26	0.25923774	23.4	36.1

Supplemental Figure 4 (Related to main Figure 4). *Nfl* deficiency alters normal circadian oscillations of calcium. (A) Schematic depiction of the calcium cycling assay of mammalian astrocytes. 24 hr after 1µM dexamethazone (Dex) treatment of control and *Nfl* deficient cells (*Nfl-/-* astrocytes), the cells were incubated with Cal 520 (4µM) solution for 2 hours before sampling at the time points indicated for two days. (B) Highly magnified fluorescence images of a time-course of changes in calcium in wild-type (Control; upper panels) and *Nf1-/-* astrocytes (lower panels) after dex stimulation. Images were taken with FITC (474nm excitation and 530 nm emission) and Dapi (350nm excitation and 470nm emission) filter sets. Dapi-merged images are shown in parallel to indicate cell nuclei. Scale bar: 20µm (C) Quantitative measurement of calcium in individual wild-type (Control) or *Nf1-/-* astrocytes shown in Figure 4. Original green fluorescent images of cells were converted to white and black mode, cells with calcium signals were demarcated (yellow dashed lines) and the intensity of the signal was quantified using Image J software. (D) JTK_CYCLE and Lomb-Scargle (LS) analysis of the calcium cycling dataset shown in Figure 4 using Meta-cycle R program (Wu et al., 2016). JTK cycle analysis revealed a significant rhythm in wild type (P: 5.36E-21) and *Nf1* (P: 0.01945) samples, but an advanced phase and lower amplitude in the latter (24.1399 in wild type versus 8.65 in *Nf1*). LS only detected a rhythm in wild type, but not in *Nf1* mutant flies. BH.Q: q-value estimated by the Benjamini-Hochberg procedure.